JOINT EUROPEAN TORUS

JET–P(88)51

V.P. Bhatnagar, J.G. Cordey, J. Jacquinot, D.F.H. Start
and JET Team

Effect of Sawteeth, Safety Factor and Current on Confinement during ICRF Heating of JET

Effect of Sawteeth, Safety Factor and Current on Confinement during ICRF Heating of JET

V.P. Bhatnagar, J.G. Cordey, J. Jacquinot, D.F.H. Start
and JET Team*

JET-Joint Undertaking, Culham Science Centre, OX14 3DB, Abingdon, UK

** See annex of P. Lallia et al, "Plasma Heating in JET",*
(13th EPS Conference on Controlled Fusion and Plasma Physics, Schliersee, Germany (1986)).

Preprint of Paper to be submitted for publication in
Plasma Physics and Controlled Fusion

Table of Contents

Abstract

The plasma stored energy as a function of input power follows an off-set linear law during ion-cyclotron resonance heating in the JET tokamak. The behaviour of experimentally obtained incremental confinement time τ_{inc} of centrally heated ICRH discharges is understood in terms of a local heat transport model where $\chi_0 \propto I_p^{-1.2}$ and that $<\chi>$ increases as the size of the $q = 1$ surface is increased at higher I_p / B_t or lower q_a due to the presence of the sawtooth instability, where I_p is the plasma current, B_t is the toroidal field and q_a is the tokamak safety factor at the plasma edge. With the transient stabilization of sawteeth by central ICRF heating in JET, we are also able to assess the effect of sawteeth on confinement and determine the plasma current scaling of τ_{inc} without mixing its dependence on the safety factor. The same model is also used to explain the degradation of τ_{inc} when ICRH power is deposited off-axis.

1.0 INTRODUCTION :

Global energy confinement time ($\tau_G = W/P_T$) in tokamaks is observed to decrease as the additional heating such as ion-cyclotron resonance heating (ICRH) or neutral-beam injection (NBI) heating power is raised. Such a behaviour is often bench-marked against the confinement scaling ($T_G \propto I_p\ P_T^{-1/2}$) deduced by Goldston (Goldston, 1984) by analyzing the NBI heating data of a number of tokamks operating in the early nineteen-eighties. In the above, W represents the plasma stored energy, P_T: the total input power and I_p: the plasma current. However, many tokamak experiments such as JET (Jacquinot, 1988), D-III-D (Burrel, 1984), TEXTOR (Messiaen,1985), JFT-2M (Odajima, 1986) show that the stored energy increases roughly linearly with the additional heating power but the straight line does not go through the origin indicating again a degradation in confinement time from the initial heating (or OH) level. Such a behaviour is generally referred to as the "off-set linear" law of confinement. The power law mentioned above implies that the confinement would continue to degrade as the input power is raised whereas the off-set linear law indicates the confinement will reach an asymptotic value (see below) and is thus relatively more optimistic. This off-set linear behaviour is also predicted by the theoretical heat-pinch (Callen, 1987) or the critical temperature gradient model (Rebut, 1986, Lallia, 1988). In these formulations, the total stored energy can be written as

$$W = W^0 + \tau_{inc}\ (P_T - P^0) \qquad (1)$$

where W is the initial plasma energy (or W_{OH}) and P^0 is the initial heating power (or P_{OH}). Thus we can define an "incremental" confinement time given by the slope of the above line which does not degrade with the input power. We must add, however, that due to the scatter of the experimental data and the range over which this data is presently available in tokamaks, the power law can also fit the data. But, the heat-pulse propagation studies in JET (Tubbing, 1987) show that the heat diffusivity χ_e derived from such measurements does not increase with the additional heating power and is, therefore, consistent with the off-set linear behaviour of stored energy. These χ_e measurements, therefore, do not appear to support the power law (Goldston, 1984) which predicts that χ_e should increase with the square-root of the heating power.

As the additional heating power is continued to increase, one is expected to arrive asymptotically to a situation such that $W >> W^0$ and the τ_{inc} would replace τ_G. Therefore, with a view to assessing the performance of a future tokamak reactor, it is of relevance to study the scaling of incremental confinement time. Such studies in TEXTOR indicate that auxiliary heating confinement time (for definition, see Vandenplas, 1986, but $\tau_{inc} \approx \tau_{aux}$ when $\Delta P_{OH} = \Delta N_e = 0$) increases linearly with plasma current. However, a different scaling is advocated by

Shimomura (Shimomura, 1987) in which τ_{inc} is independant of I_P and it mainly depends on the minor radius a_p of the tokamak plasma giving a scaling as τ_{inc} (s) $= 0.12\ a_p^2$(m).

In this paper, our efforts are directed to confinement scaling studies based on the experimental results obtained in the JET tokamak with ion-cyclotron resonance heating. The dependence of τ_{inc} on plasma current and the tokamak safety factor q has been studied by varying I_P from 1 to 6 MA, q_{cyl} (cylindrical q) from 1.8 to 6. The effect of off-axis power deposition profile on τ_{inc} has also been investigated. With the production of "Monster" or ultralong sawteeth (duration greater than the energy confinement time) in JET, we are also able to assess the effect of sawteeth on confinement.

We find that τ_{inc} improves with I_P at low currents (1-2 MA), saturates and subsequently degrades at higher currents (4-6 MA). These results are compared with a local heat transport model which assumes that χ (where $\chi \propto 1/\ \tau_{inc}$, see below) depends on two competing mechnisms, that is, it decreases with I_P but increases as the size of the $q = 1$ surface increases at higher I_P/B_T or low q_{cyl}. The experimentally observed degradation of τ_{inc} when the ICRH power is deposited off-axis is also discussed in terms of the above model. There is a modest improvement (see below) in τ_{inc} derived from the stored energy deduced from the diamagnetic measurements for discharges featuring monster sawtooth over the non-monster case. This is related to the fact that fast ions in JET are well confined, (which may stabilise the sawtooth instability (Coppi, 1988, White, 1988)), and result in improvement of stored energy whereas frequent sawteeth redistribute them away from the core, periodically losing a fraction of their contribution to stored energy.

The paper is organised as follows. In section 2, we present the experimental results on incremental confinement time for a range of I_P and q_{cyl} values as well as the data with off axis heating. Also in this section we compare the τ_{inc} values of discharges with and without monster sawtooth. The local heat transport model (Callen, 1987) is then outlined in Section 3 and the predictions based on this model are compared to the experimental results. Discussion and conclusions of this study are contained in Section 4.

2.0 EXPERIMENTAL RESULTS :

JET (Joint European Torus) is a D-shaped large tokamak (Bickerton, 1987) with major radius R_0 = 2.96 m, minor radius a_p = 1.2 m, nominal toroidal field B_t = 3.4 T, plasma current I_p = 5 MA (upgraded to 7 MA), and plasma elongation = 1.6. For the results presented in this paper, we include the ICRH data obtained in JET limiter discharges. Some data of X-point (Tanga, 1986) L-mode discharges has also been incorporated to extend the range of plasma current down to 1 MA where limiter data was not available.

The JET ICRH system has been described previously (Wade,1985 ; Kaye, 1987). In the early ICRH experiments (1985-86) on JET, three (A_{01},A_{02}) antennas (see Wade, 1985) located on the low field side of the tokamak were used. These have been replaced by eight A_1 antennas (see Kaye, 1987) which are symmetrically distributed around the torus. A JET antenna has essentially two radiating elements that are separated toroidally which can be driven in phase (monopole) or out of phase (dipole). In monopole operation, the antenna radiated power spectrum is centered at k// = 0 with a half width of 4.5 /m whereas in dipole operation k// = 7 /m and the half width is 3.5 /m. An electrostatic screen made out of nickel is used to filter out the slow wave. ICRH power is delivered to the plasma by coupling the fast magnetosonic wave which deposits its power mainly via the minority-ion cyclotron damping in a narrow region (about 30 cm) near the ion-ion hybrid resonance zone (Jacquinot, 1986). Most of the RF power (up to 70 %) first appears in the fast minority ions that have strong perpendicular anisotropic tail which subsequently relaxes on the electrons. Direct electron heating is about 5 to 10 % in the H-minority case whereas it is about 10 to 30 % in He-3 minority case (Jacquinot, 1988). The range of plasma parameters under ICRF heating are given in Table 1.

2.1 Off-Set Linear Behaviour :

A plot of stored energy (from diamagnetic measurements) W_D vs. P_T- $\dot{W}_D$ is illustrated in Fig. 1 for different I_p as indicated where P_T is the total input power and the dot refers to the time derivative. The measured W_D also includes the significant perpendicular energy that is carried by the fast ions created during the minority heating which are well confined in JET and their contribution to W_D is estimated to be typically 15 %. It is seen from Fig. 1 that W_D follows an off-set linear law. The τ_{inc} is determined by the slope of a line which is least square fitted to the data points for the power scan at a given I_p. We note that τ_{inc} (D) increases with I_p up to 3 MA but it is lower at 5 and 6 MA. Here D refers to the diamagnetic stored energy.

The τ_{inc} values both from W_D and W_e (electron kinetic energy) obtained from such scans at these and other currents are plotted in Fig. 2 as a function of I_p. The W_e is calculated from n_{e0}, T_{e0} and integration over the profiles. It is seen that τ_{inc} (e) first increases with I_p, saturates and then decreases with I_p. Similar behaviour is also found for the τ_{inc} (D) obtained from a series of shots that did not feature monster sawteeth. The remaining τ_{inc} (D) points in Fig. 2 appear to be slightly better which were obtained from power scans in which some shots produced monster sawteeth. The superior values in the latter case are presumably due to the larger contribution of the fast ions to stored energy as will be discussed below. Note that the present L-mode X-point and limiter ICRH discharges give about the same τ_{inc} values. Also, the second harmonic heating ($2\ \omega_{ch}$) data point compares well with the other data. A comparison of this data to model calculations will be presented Section 3.

2.2 *Dependence of Incremental Confinement Time on q :*

The τ_{inc} data shown in Fig. 2 is now plotted in Fig. 3 as a function of I_p/B_t where this quantity is inversely proportional to q_{cyl} if the plasma cross sectional area is held constant (for typical values of JET plasma cross section $q_{cyl} = 3.3\ (I_p/B_t)^{-1}$). It is seen that maximum τ_{inc} is found when $I_p/B_t \approx 1$ which is $q_{cyl} = 3.3$. The data points are again identified with respect to current as in Fig. 2. This data has also been plotted (not presented here) as a function of q_{cyl} and the behaviour is roughly the same as in Fig. 3 with the maximum in τ_{inc} appearing at $q_{cyl} \approx 3.3$.

2.3 *Effect of Off-Axis Heating :*

The ICRH data presented in Figs. 1-3 corresponds to central heating where the minority ion cyclotron layer (R_c) was located close to the magnetic axis near which most of the RF power is absorbed. In order to assess the effect of off-axis heating on confinement, we have carried out ICRH experiments where R_c was moved off-axis from the center to about 2/3 of the plasma radius on the outboard side. At each position of the minority ion (H^+) cyclotron layer, a number of shots are made by varying the ICRH power and the plasma stored energy is measured. In Fig. 4, we plot W_D as a function of P_T for discharges with $I_p = 2$ MA where the time derivative of W_D is less than 10 %. The data taken with majority deuterium or He-3 gas and the locations of R_c have been identified in Fig. 4. The values of τ_{inc} obtained from Fig. 4 is now plotted in Fig. 5 as a function of the cyclotron layer position from the magnetic axis. The cyclotron layer position has been calculated (Bhatnagar, 1987) by taking paramagnetic contribution to B_t, the poloidal field and the effect of poloidal beta (β_p) in to account. Note that the incremental confinement time is practically the same when R_c is moved from the axis to about 40 cm off-axis. However, a clear degradation in the slope (see Fig. 4) is found when the R_c is displaced more than 40 cm from the axis. Note that for the data of discharges plotted in Figs. 4-5, q_{cyl} was about 3.5 from which the mixing radius (for definition see for example (Tubbing, 1987)) r_m (the JET experimental data fits a relation $r_m \approx 1.4/q_{cyl}$ approximately) is estimated to be about 40 cm. Thus it appears from the data that there is little enhanced degradation in τ_{inc} when the power is deposited off-axis but that lies within the mixing radius. However, a clear enhanced degradation of τ_{inc} is found when the

power is deposited extreme off axis such that it lies outside r_m (see for example Esiptchuk, 1986, for similar off-axis but electron cyclotron heating results on T-10 tokamak). The former behaviour is predominantly dictated by the existence of a strong heat diffusion within the mixing radius brought about by the sawtooth instability. However, the latter behaviour is governed by the higher heat diffusion that prevails in the outer region of the plasma. A model which assumes a χ_e (r) variation consistent with what is used in transport analysis (Taroni, 1985, Behringer, 1984) to simulate the sawtooth phenomenon will be used in Section 3 to predict τ_{inc} values and will be compared with data of Fig. 5.

2.4 Effect of Monster Sawteeth :

We now compare the τ_{inc} deduced from certain scans where we have sorted the plasma discharges with and without the occurence of monster sawtooth. The τ_{inc} values obtained from such scans are plotted in Fig. 6 as a function of I_P and the data points are identified as shown. It is found that on average, there is about 10-15 % improvement in τ_{inc} (D) with monster over the non-monster case. Note that there is practically no improvement in τ_{inc} (e) on a similar comparison. The modest amelioration in τ_{inc} (D) with monster sawteeth is related to the fact that fast ions produced during the minority RF heating scenarios in JET remain well confined during a monster sawtooth and result in improvement of diamagnetic-loop measured stored energy whereas frequent sawteeth redistribute the fast ions away from the core, periodically losing a fraction of their contribution to stored energy. The monster sawteeth thus show their importance in reactor environment in preventing the ejection of α-particles from the core due to frequent sawteeth crashes.

2.5 Scaling with Plasma current :

Generally, monster sawteeth are produced in discharges with $I_P / B_t \approx 1$ (or $q_{cyl} \approx 3.3$). The toroidal field in JET is limited to 3.5 T, therefore, the τ_{inc} data with monster sawteeth in Fig. 6 is limited to 3.5 MA. We must add that occasional monster sawteeth have been obtained at 4 and 5 MA but, there are no scans under such conditions to deduce τ_{inc} at these currents. The τ_{inc} data with monster sawteeth shown in Fig. 6 range from 1.5 to 3.5 MA but q_{cyl} lies in the limited range of 3 to 3.3. Moreover, for this data, the ICRH frequency was adjusted such that the RF power was deposited near the magnetic axis. We point out that monster sawteeth could not be produced by off-axis ICRF heating. Thus, the data of Fig. 6 can be considered to be at a fixed value of q_{cyl} and with central heating. From this data, we can therefore determine the current scaling of incremental confinement time. The broken lines drawn through the points shows a variation of $\tau_{inc} \propto I_P^{1/2}$. This square-root current dependance of τ_{inc} will be included in the next section when modeling the behaviour of τ_{inc} with current, safety factor q and off-axis heat deposition during ICRF heating of JET.

3.0 MODELING :

The total heat flux q through the confinement zone, deduced from the measurements in JET discharges, has previously been shown (Cordey, 1986) to fit the following form

$$q = - n \chi \text{ grad } T - q_0 \qquad (2)$$

where χ is the heat diffusion coefficient and the two terms on the right-hand side represent the heat conduction and convection respectively. Further, the convective term q_0 is found to be negative (Cordey,1986) which indicates a heat pinch or critical temperature gradient onset phenomenon (Rebut, 1986, Lallia, 1988). We must add that at present no clear evidence exists which would describe the mechanism for such a heat pinch. Utilising the above expression in the equilibrium heat balance equation, one obtains the temperature gradient, temperature profile and the stored energy W by successive integrations (Cordey, 1986; Callen, 1987). If χ and q_0 are practically independent of T, grad T and input power, an expression for stored energy can be written as (Cordey,1986)

$$W = \tau_{inc} P_{in} + W^0 \qquad (3)$$

where $\tau_{inc} = \tau_\chi . \eta$ and where $\tau_\chi = 3 \text{ ab} / 4 < \chi >$ represents an ideal incremental confinement time if there was no degradation due to profile effects (see below). Note that $< \chi >$ is a spatially averaged (see Callen, 1987) heat diffusivity and a and b are the radii of an elongated plasma in the horizontal and the vertical direction respectively. The subscript p from a has been dropped for convenience. The symbol η represents the heating "effectiveness" of the input power in which the account is taken of radiated power and the profile effects of the ohmic and that of auxiliary heating power deposition (Callen, 1987). Since the power radiated in JET predominantly originates from the outer 1/3 of the plasma, we shall neglect its effect on confinement. Also, in the following, the heating effectiveness of the OH power is taken to be unity, but, the heating effectiveness of ICRH power will appropriately be taken into account with the idealization that it is unity for delta-function heating at the plasma centre (or effectively anywhere inside the mixing radius) and zero for delta-function heating at the plasma edge (Callen, 1987). In the experiment, the ICRH power deposition profile is not a delta-function, nevertheless, it is relatively narrow when compared to the plasma radius of JET (Jacquinot,1986).

Though χ and q_0 were assumed to be independent of T, grad T or input power but, χ is still a function of radial position. The spatial dependence of $\chi(r)$ will be used below to model the effect of sawteeth and off-axis ICRF heating profiles on the incremental confinement time.

A radially increasing χ has been inferred in many tokamak experiments from local power balance analyses (see for example Hughes, 1978, Berzilov, 1983 and Efthimion, 1984). Therefore, we assume that

$$\chi(r) = \chi_0 / (1 - \alpha\, r^2/a^2), \quad \alpha < 1. \tag{4}$$

The periodic central temperature profile flattening due to sawteeth can be modelled by defining an equilibrium $\chi(r)$ that is infinitely large inside the sawtooth mixing radius r_m and a $\chi(r)$ given by the expression (4) outside the mixing radius.

This gross general variation of $\chi(r)$ is also used in transport code simulations (Taroni, 1985, Behringer, 1984) of sawteeth phenomenon. such a spatial dependence of $\chi(r)$ leads to (Callen, 1987)

$$<\chi> \;=\; 2\chi_0 / \{(1 - (r_m/a)^2).(1 - \alpha/2\,(1 + (r_m/a)^2))\} \tag{5}$$

If the RF power is deposited within the mixing radius, the effect of changing q_{cyl} or r_m on ideal incremental confinement time can be described by the following formula

$$\tau_\chi = 3\,ab / 4<\chi> \tag{6}$$

where $<\chi>$ is given by Eq. (5). If the RF power is deposited beyond the mixing radius, the heating efficiency is given by (Callen,1987)

$$\eta = 1 - (r_h/a)^2.(1 - (\alpha/2).(r_h/a)^2) / (1 - \alpha/2) \tag{7}$$

where r_h is the location of the delta function heating power deposition. Assuming $\chi_0 \propto I_p^{-\beta}$ and for simplicity taking $\alpha = 1$, the incremental confinement time can be written to fit the experimental data as

$$\tau_{inc}(s) = \tau_{inc0}(s) \,.\, \eta \,.\, I_p^{\beta}(MA) \,.\, (1 - (r_m/a)^2)^2 \tag{8}$$

where

$$\eta = (1 - (r_h/a)^2)^2 \qquad \text{for } r_h > r_m \tag{9}$$

and

$$= 1 \qquad \text{for } r_h < r_m$$

and $\tau_{inc0} = 3\,ab/8\chi_0$. In the expression (8), τ_{inc0} and β can be adjusted to fit the experimental data.

We are now in a position to compare the predictions based on the model outlined above to the experimental results presented in Section 2. First, we note that the expression (3) represents the off-set linear behaviour described by the experimental data shown in Fig. 1. The expression (8) can be used to describe the behaviour of τ_{inc} such as that shown in Fig. 2 and 3 if the value of τ_{inc0} and β is known. As we pointed out in Section 2 and shown in Fig. 6 the value of $\beta = 1/2$

can be used from JET results. Since there are no definite experimental results which provide the value of χ_θ, we choose to fit the prediction to one experimental point and compare the behaviour of τ_{inc} as I_p/B_t (or q_{cyl}) and as the location of the heating profile is changed. Since τ_{inc} is a function of I_p, r_m (or q_{cyl}) and r_h, a single curve can not be compared to the experimental data. Instead, a point by point comparison has to be made. For clarity, we show fitted points (solid diamonds) for τ_{inc} (e) only in Fig 2 and 3 which should be compared with triangles. These are found to be in fairly good agreement assuming $\tau_{inc0} = 0.14$ s. Note that for the data shown in Fig. 2 and 3, r_h was located within the mixing radius, hence $\eta = 1$ has been used.

The behaviour of τ_{inc} with the location of heat deposition within the mixing radius or outside r_m is also very well described by the above model (see Eq. (9)). The experimental data in Fig. 5 shows that τ_{inc} changes very little when the power deposition is within the mixing radius whereas degrades significantly when it is outside r_m.The broken line drawn in Fig. 5 represents the variation prescribed by Eq.(9) for $r > r_m$.

4.0 DISCUSSION AND CONCLUSIONS :

The incremental confinement time can, in principle, be deduced from a single shot by computing the quantity $\triangle W/\triangle P_T$, but there may be a significant shot-to-shot variation depending upon the power level (especially at lower power) and the accompanied change of density. The importance of the error due to the change of density is reduced if τ_{inc} is obtained from the slope of the W vs. P_T graph (as is done here) since the density rise levels off as the RF power is increased. However, often the τ_{inc} obtained at different plasma currents pertains to different operating densities. The higher operating densities at higher currents generally lead to a larger off-set in the W vs P_T plot, but, the slope of the line (or the τ_{inc}) is affected very little. If the power scans at different currents are made strictly at constant density, though this is very tedious in the experiment, it is possible that we find the value of β slightly higher than 1/2 which is used to fit the data here. Furthermore, at higher densities, the fast-ion component is likely to be smaller than that at lower operating densities which may lead to lower τ_{inc} (D) (that of diamagnetic stored energy) but τ_{inc} (e) (electron energy) is expected to remain unaffected.

The effect of radiated power can be systematically taken into account when plotting W vs. P_T data (Cordey,1986) but we have for simplicity restricted to low radiated power data such that $P_{rad}/P_T < 0.5$. Though the heating effectiveness of ohmic heating power deposition profile is taken to be unity, it is expected to be about 0.85 (Cordey,1986) and which would improve τ_{inc} by about 15 %. In the modeling, ICRF heating power deposition profile is taken to be a delta-function whereas in practice it has a width of about 0.3 m (Jacquinot, 1986) when the plasma radius of JET is 1.2 m. The appropriate account of the finite width of power deposition is likely to lower a little the value of α from unity that is used in fitting the data (Callen, 1987).

In conclusion, we find that during ion-cyclotron resonance heating in the JET tokamak, the stored energy as a function of total input power follows an off-set linear behaviour indicating a degradation in confinement from initial (or OH) level. The confinement does not continue to degrade with the input power as predicted by the power law, but asymptotically it is given by the slope of the off-set line referred to as the incremental confinement time τ_{inc}. The behaviour of experimentally obtained τ_{inc} of centrally heated ICRF discharges as shown in Figs. 2 and 3 is understood in terms of a local heat transport model where the heat diffusion coefficient $\chi_0 \propto I_p^{-\beta}$ and that $<\chi>$ increases as the size of the q = 1 surface (or more appropriately the mixing radius) increases at higher I_p / B_t or lower q_{cyl}. This is related to the effect of the sawtooth instability which enhances the diffusion coefficient strongly within the mixing radius. Consistent with the same model, where it is assumed that χ is infinitely large within r_m and

increases approximately parabolically outside r_{m_i} the effect of off-axis ICRF heating profiles on τ_{inc} is negligible if the power is deposited within the mixing radius, but, there is significant degradation in τ_{inc} (given by Eq. (9)) when the power is deposited outside r_m. In examining discharges which feature monster sawtooth (duration greater than the energy confinement time), it is found that they generally occur when $3 < q_{cyl} < 3.5$ (or $I_p / B_t \approx 1$) and the power deposition has to be near the axis. The study of τ_{inc} of monster sawtooth discharges (narrow range of q_{cyl} and central power deposition) allows us to assess the scaling of τ_{inc} with plasma current which is found to be approximately a square-root dependence. Finally, the loss of fast particles by sawteeth is a significant energy loss which is avoided in a monster sawtooth discharge.

5.0 ACKNOWLEDGEMENT :

We wish to thank our colleagues in the JET team, especially the RF plant and the tokamak operation teams and those operating the diagnostics used in the experiments reported in this paper. Helpful discussions with R. Bickerton, D. Campbell, J.D. Callen, A. Taroni, P.R. Thomas and K. Thomsen are highly appreciated. The support of J.J. Ellis in computer codes used for data analysis is greatefully acknowledged.

6.0 REFERENCES :

(1) Bhatnagar, V.P., (1987), JET-JDN(87)3, Internal Note, JET Joint Undertaking, Abingdon, Oxon, England (unpublished).

(2) Behringer, K.H. et al, (1984), Proc. IAEA Conf. on Plasma Phys. and Controlled Nuclear Fusion Research, London, (U.K.), Nuclear Fusion Supplement 1985 , Vol. 1, 291.

(3) Berzilov, A.B. et al, (1982) Proc. IAEA Conf. on Plasma Phys. and Controlled Nuclear Fusion Research, Baltimore, (U.S.A.), Nuclear Fusion Supplement 1983 , Vol. 2, 63.

(4) Bickerton, R.J. et al, (1987) Plasma Phys. and Controlled Fusion, 29, 10A, 1219.

(5) Burrel, K.H. et al, (1984), Proc. IAEA Conf. on Plasma Phys. and Controlled Nuclear Fusion Research, London, (U.K.), Nuclear Fusion Supplement 1985 , Vol. 1, 131.

(6) Callen, J.D., Chritiansen, J.P., Cordey, J.D., Thomas, P.R., Thomsen, K., (1987) Nucl. Fusion 27, 1857.

(7) Coppi, B., Hastie, R.J., Migliuolo, S., Pegoraro, F., Porcelli, F., (1988), JET-P(88)20, JET Joint Undertaking, Oxon, England, to be published in Physics Letters A.

(8) Cordey J.G. et al (1986), Proc. IAEA Conf. on Plasma Phys. and Contr. Nuclear Fusion Research, Kyoto, Japan, Nuclear Fusion Supplement 1987, vol. 1, 99.

(9) Efthimion, P.C. et al, (1984) Proc. IAEA Conf. on Plasma Phys. and Controlled Nuclear Fusion Research, London, (U.K.), Nuclear Fusion Supplement 1985 , Vol. 1, 29.

(10) Esiptchuk, Yu.V., Razumova, K.A.,(1986), Plasma Phys. and Controlled Fusion, 28, Number 9A, 1253.

(11) Goldston (1984) , Plasma Phys. Controlled Fusion 26, 87.

(12) Hughes, M.H. and Hugill, J.,(1978), Proc. IAEA Conf. on Plasma Phys. and Contr. Nuclear Fusion Research, Innsbruck, Austria, Nuclear Fusion Supplement 1979, vol. 1, 457.

(13) Jacquinot, J. et al (1986), Proc. IAEA Conf. on Plasma Phys. and Contr. Nuclear Fusion Research, Kyoto, Japan, Nuclear Fusion Supplement 1987, vol. 1, 449.

(14) Jacquinot, J. et al, (1988), Invited Paper, 15th European Conf. on Controlled Fusion and Plasma Physics, (to be published in Plasma Phys and Controlled Fusion).

(15) Kaye, A.S. et al (1987), Fusion Technology, 2, 203.

(16) Lallia, P.P. et al, (1988), JET-P(88)05, Preprint, JET Joint Undertaking, Abingdon, Oxon, England (unpublished).

(17) Messiaen, A.M. et al, (1986) Plasma Phys. and Controlled Fusion, 28, 1A, 204.

(18) Odajima, K., et al, (1986) Phys. Rev. Letters, 57, 2814

(19) Rebut, P.H., Brusati, M., Hugon, M., Lallia, P.P. (1986) Proc. IAEA Conf. on Plasma Phys. and Contr. Nuclear Fusion Research, Kyoto, Japan, Nuclear Fusion Supplement 1987, Vol. 3, 187.

(20) Shimomura, Y. and Odajima, K. (1987), Comments Plasma Phys. and Controlled Fusion, 10, 207.

(21) Tanga, A. et al, (1986), Proc. IAEA Conf. on Plasma Phys. and Contr. Nuclear Fusion Research, Kyoto, Japan, Nuclear Fusion Supplement 1987 , Vol. 1, 65.

(22) Taroni, A., Tibone, F. (1985), JET-DN-T(85)7, Internal Note, JET Joint Undertaking, Abingdon, Oxon, England (unpublished).

(23) Tubbing, B.J.D., Lopez Cardozo, N.J., (1987) Nuclear Fusion, 27, 1843.

(24) Vandenplas, P. et al (1986), Proc. IAEA. Conf. on Plasma Phys. and Contr. Nuclear Fusion Research, Kyoto, Japan, Nuclear Fusion Supplement 1987 , Vol. 1, 485.

(25) Wade, T. et al (1985) Proc. 11th Symposium on Fusion Engineering, Austin, Texas.

(26) White, R.et al, (1988), Phys. Rev. Letters, 60, 2038.

TABLE 1. RANGE OF JET PLASMA PARAMETERS UNDER ICRF HEATING

Parameters	Range
ICRH Power (MW)	0 - 16
RF Frequency (MHz)	25 - 52 (in steps)
Toroidal Field (T)	2 - 3.5
Plasma Current (MA)	1 - 6
OH Power (MW)	0.7 - 4.5
Average Plasma Density (m^{-3})	$2 - 5 \times 10^{19}$
Central Electron Temperature (keV)	2 - 10
Cental Ion Temperature (keV)	2 - 7.5
Fraction of Radiated Power to Total Input Power	0.2 - 0.5
Plasma Effective Charge	2 - 5

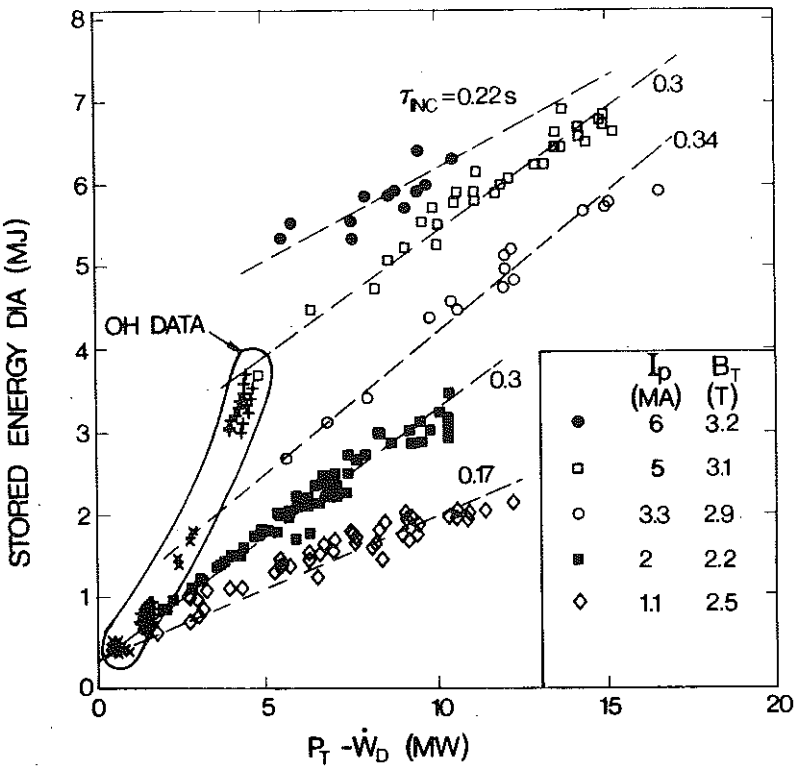

Fig. 1 A plot of the stored energy W_D (diamagnetic measurements) as a function of $P_T - \dot{W}_D$ at different plasma currents where P_T is the total input power (OH + ICRH) and the dot refers to the time derivative. The data refers to the limiter discharges except that at 1.1 MA which are for X-point L-mode discharges.

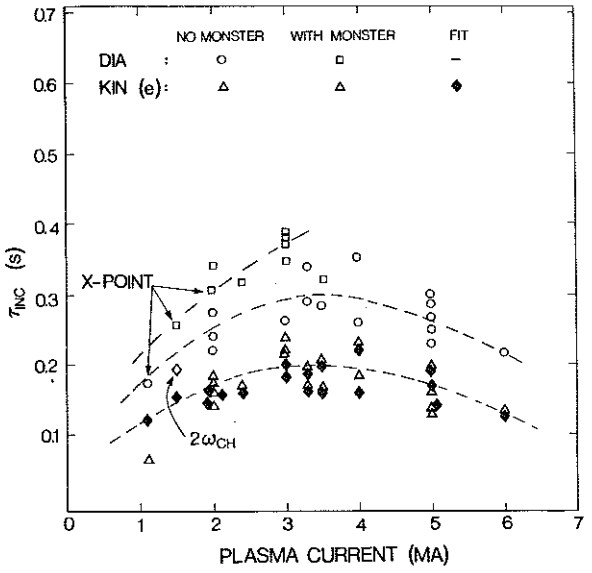

Fig. 2 The incremental confinement time plotted as a function of discharge current. Each point refers to a power scan such as that shown in Fig. 1. Several scans at a given current were made with different B_t thus referring to different I_p/B_t or q_{cyl}. The data is for limiter discharges except the points shown for single-null X-point discharges. The ICRH data is obtained under minority-ion heating scheme except the $2\omega_{CH}$ point which refers to the second harmonic heating in hydrogen plasma. The data 'with monster' was obtained with power scans in which some shots produced monster sawtooth and others had regular sawteeth. Same symbol has been used for τ_{inc}(e) with or without monster sawteeth as there is practically no difference among them. Note that the data with monster is restricted to I_p below 3.5 MA. The fit refers to Eq. 9 and the comparison is only shown with τ_{inc}(e) obtained from electron kinetic energy.

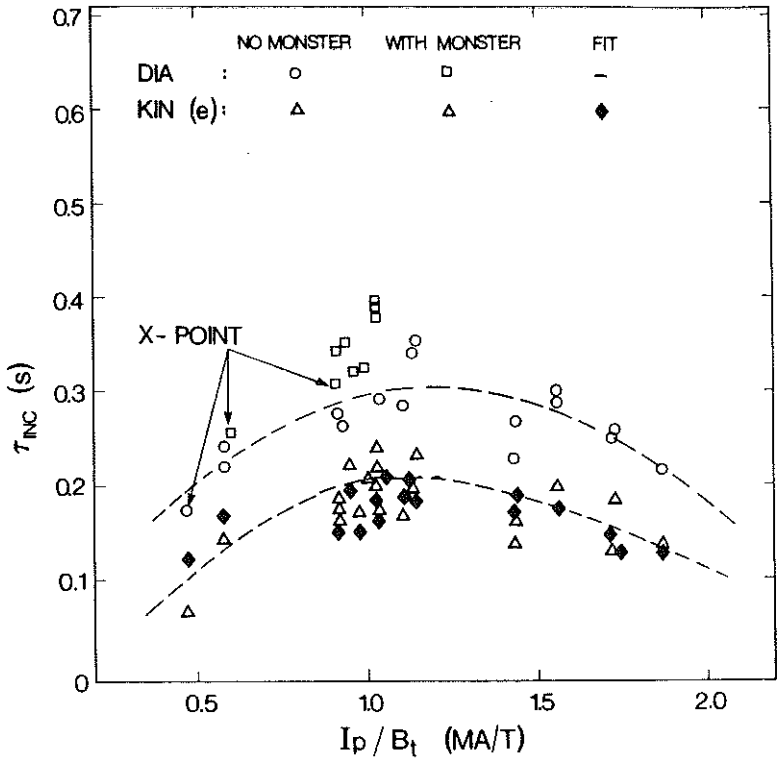

Fig. 3 The τ_{inc} data shown in Fig. 2 is plotted as a function of I_p/B_t. See also remarks mentioned in Fig. 2.

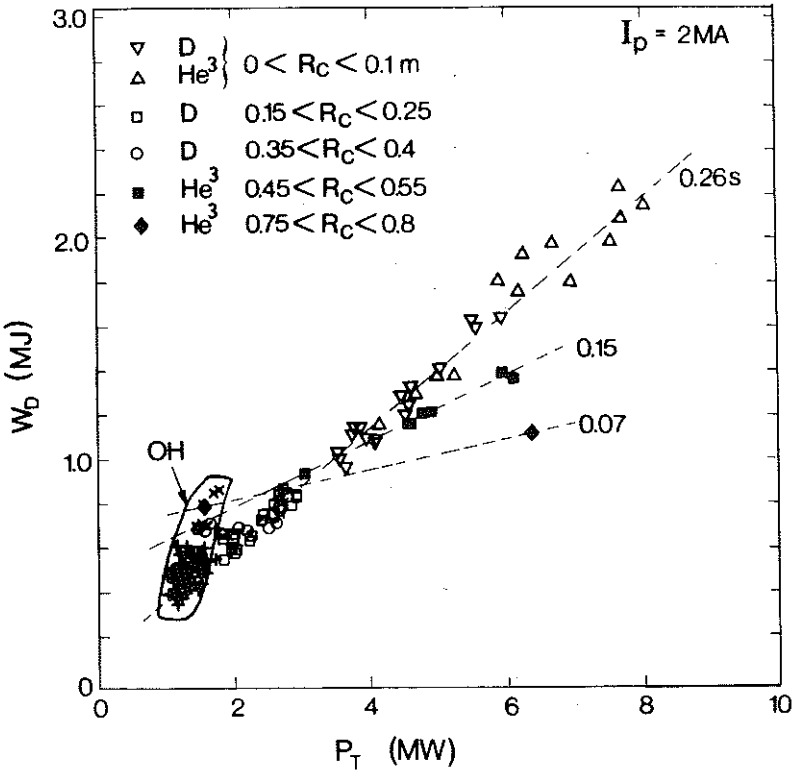

Fig. 4 A plot of W_D as a function of total input power for discharges at 2 MA where the minority-ion cyclotron layer (R_c) position was changed in a range as indicated in the figure. The symbols D, ^{3}He etc. refer to the majority plasma gas whereas the minority species was hydrogen.

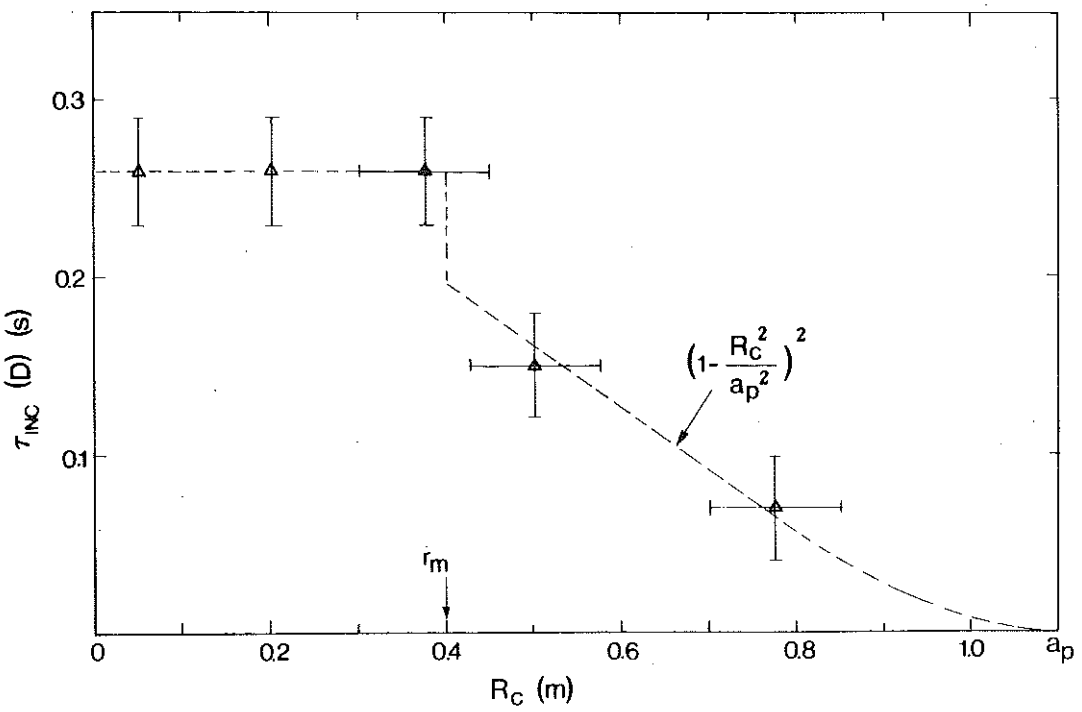

Fig. 5 The τ_{inc} values obtained from the scans of Fig. 4 are plotted as a function of the cyclotron layer position which is roughly the ICRH power deposition region. The expected variation from the model outlined in section 3 is shown with the broken line

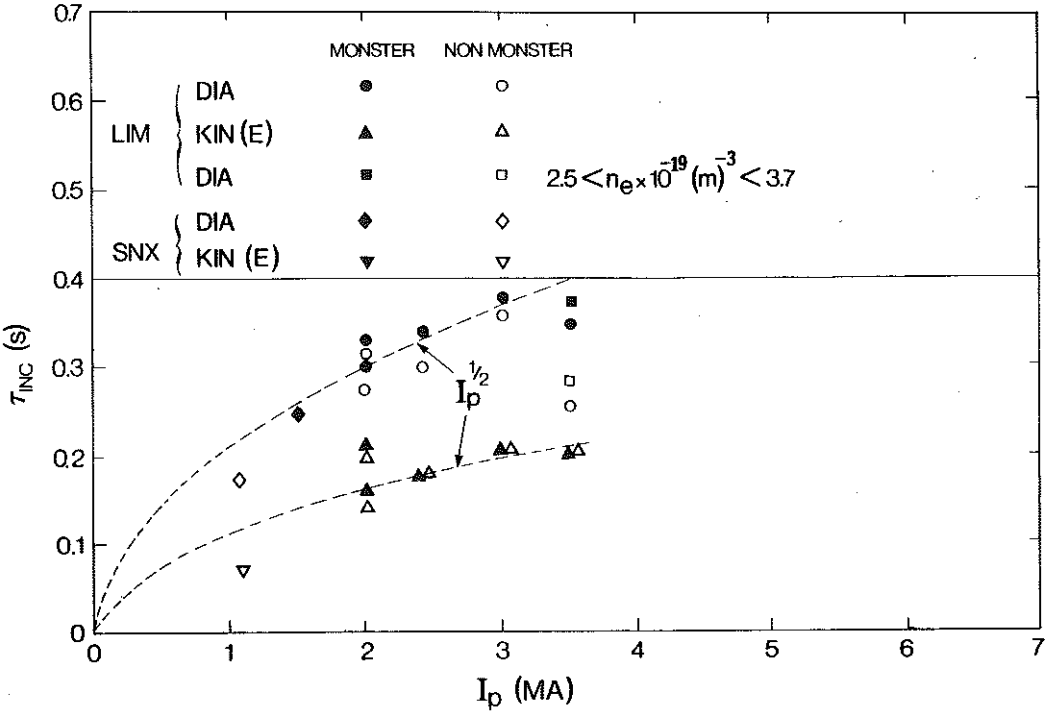

Fig. 6 A plot of τ_{inc} as a function of I_p where the power scan data points were sorted with discharges with or without monster sawtooth. SNX refers to single null X-point discharges. The broken lines represent square-root current dependence. The data shown refers to a narrow range of q_{cyl} values and central RF power deposition.